

# Electronic level structure and density of states of a terminated biperiodic superlattice

R. Kucharczyk\* and M. Stęślicka

*Institute of Experimental Physics, University of Wrocław, plac Maksa Borna 9, 50–204 Wrocław, Poland*

B. Djafari-Rouhani

*Laboratoire de Dynamique et Structure des Matériaux Moléculaires, UPRESA CNRS No. 8024, UFR de Physique, Université de Lille I, 59655 Villeneuve d'Ascq Cedex, France*

(Received 30 November 1999)

Electronic level structure and density of states (DOS) of a biperiodic superlattice (SL), whose period consists in general of two arbitrary wells coupled via two different barriers (the so-called double-well basis), is investigated with emphasis placed on surface effects due to SL termination by a substrate or a cladding layer. Special attention is paid to the possibility for surface states, i.e., the states confined to the SL/substrate interface, to exist within SL minigaps. Dependence of their properties (i.e., the energy position and the degree of localization) on the choice of substrate is studied for various terminating configurations (depending on the sequence of SL layers approaching the surface) of an AlGaAs-based double-well SL. Surface-induced modifications of extended states forming SL minibands are also discussed, indicating a possibility to arrange—in a controlled manner—different local DOS (LDOS) distributions at the SL end. This might have important consequences for particular applications of biperiodic SL's.

## I. INTRODUCTION

The so-called polytype or complex-basis superlattices (SL's), composed of alternating layers of more than two different materials, attract recently an increasing interest connected with the search for microelectronic devices of superior characteristics. When additional layers are introduced in each SL period, more degrees of freedom in engineering the desired properties are available as compared to typical, i.e., binary (two-layer period) SL's. As a consequence, an unusual electronic structure can be realized.<sup>1–6</sup> In particular, the ability to control the miniband and minigap widths independently has proved to be of a great value for modeling infrared photodetectors, electro-optic switches and modulators of a better performance, as well as for effective-mass filtering and tuning of the tunneling current.<sup>1–3,7–12</sup>

Electronic characteristics of a polytype SL might be, however, essentially modified by surface effects due to SL termination by a substrate or a cladding layer, as it happens for binary SL's (cf. Refs. 13–15 and references therein). To address this problem, a general effective-mass approach, taking into account the existence of surface states (i.e., the states appearing within energy minigaps and confined to the SL/substrate interface) in an arbitrary multilayer-basis SL, has been recently developed<sup>16</sup> and applied next to study the surface electronic structure of a triple-constituent SL with the so-called step-well basis.<sup>17</sup> In the present paper, the energy spectrum of surface-localized states is investigated for the most commonly studied polytype SL, namely, the so-called biperiodic SL, with a general double-well geometry of the complex basis. Selected surface-state wave functions are plotted in order to illustrate their localization properties.

Moreover, since termination of a binary SL affects substantially the extended states forming SL minibands (cf., e.g., Refs. 18 and 19), a similar effect is also expected in polytype SL's. Therefore, the density-of-states (DOS) distributions at

the end of a double-well SL are additionally explored in this paper. To our best knowledge, this provides the first study of surface-induced DOS modifications in polytype SL's. Needless to say, this might be of relevance for a variety of their applications.

## II. MODEL

The structure under consideration, as schematically depicted in Fig. 1, is a semi-infinite double-well SL, described in terms of a generalized Kronig-Penney-type of model terminated by a potential step representing a substrate or a cladding layer. The SL basis consists, in general, of four layers—two arbitrary wells coupled by two arbitrary barriers—labelled with  $i = A, B, C$ , and  $D$ , of thicknesses  $d_i$ , effective-mass values  $m_i$ , and potential levels  $V_i$ , correspondingly;  $d_{\text{SL}} = d_A + d_B + d_C + d_D$  stands for the SL period. The substrate parameters are denoted by  $m_S$  and  $V_S$ .

## III. METHOD OF CALCULATION

Electronic level structure of a system is calculated using a general transfer-matrix formalism within an effective-mass

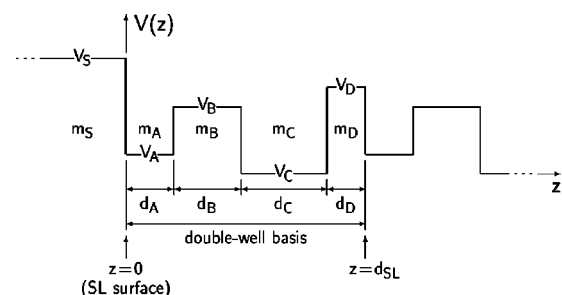


FIG. 1. Potential profile of a terminated biperiodic SL with a general double-well basis consisting of two arbitrary wells coupled via two different barriers. For notation, see the text.

approximation, described in detail in Ref. 16. Within this approach, the bulk dispersion relation as well as the energy expression for surface states can be derived—unfortunately, no concise analytical formulas can be reached for a general double-well basis, so the energy spectrum of the considered structure has to be entirely determined numerically. The respective surface-state wave functions are also computed following Ref. 16.

The DOS, in turn, is determined using a Green's-function formalism within an interface response theory, originally developed to study vibrational properties of SL's with multiple layers per period.<sup>20</sup> The closed-form expressions for local DOS (LDOS), obtained in Ref. 20 for transverse elastic waves, can be straightforwardly transposed—following Ref. 21—to treat electronic properties of biperiodic SL's within an effective-mass approximation. This enables us to compute LDOS as a function of both the electron energy  $E$  and the space coordinate  $z$ . Therefore, the space-charge distributions, associated with the localized surface states as well as the extended states forming particular SL minibands, can be illustrated in a direct way.

#### IV. RESULTS AND DISCUSSION

For numerical calculations, the AlGaAs-based SL has been chosen, as it offers a possibility to realize and manipulate a rich variety of potential profiles. More specifically, the potential level and the effective-mass value of a particular  $\text{Al}_x\text{Ga}_{1-x}\text{As}$  layer can be adjusted by the Al concentration  $x$ , e.g., according to the empirical relations  $V(x) = 944x$  meV and  $m(x) = (0.067 + 0.083x)m_{\text{el}}$ ,  $m_{\text{el}}$  being the free-electron mass (after Refs. 22 and 23). Since, however, our attention is focused here on the effects introduced by the SL surface, the bulk SL parameters have been kept fixed. Consequently, all the computations have been performed for a particular system composed of GaAs wells (i.e.,  $V_A = V_C = 0$ ) of different widths  $d_A = 40$  Å and  $d_C = 45$  Å, alternating with  $\text{Al}_{0.5}\text{Ga}_{0.5}\text{As}$  barriers (i.e.,  $V_B = V_D = 472$  meV) of different thicknesses  $d_B = 25$  Å and  $d_D = 15$  Å, which nevertheless constitutes a rather general example of a double-well basis.<sup>24</sup> This choice of SL parameters enabled us to avoid, within the considered energy range,<sup>25</sup> complications in an adequate description of minibands due to an indirect band-gap nature of the  $\text{Al}_x\text{Ga}_{1-x}\text{As}$  alloy for higher values of  $x$ . Indeed, as confirmed by our recent pseudopotential calculations,<sup>26</sup> such a biperiodic SL—as well as any two-component system, i.e.,  $A/B$ ,  $A/D$ ,  $C/B$ , and  $C/D$  binary SL's—exhibits a direct band gap, the lowest conduction minibands are clearly  $\Gamma$ -valley derived, while the  $\Gamma$ - $X$  intervalley coupling has a negligible effect on the energy spectrum of interest (see also Refs. 1, 27, and 28).

In contrast, the surface conditions—in particular, the terminating potential step  $V_S$ —have been varied assuming a changeable Al concentration  $x_S$  in the substrate. Different possible terminating configurations, depending on the sequence of SL layers approaching the surface, have also been considered. The  $V_S(x_S) = 944x_S$  meV dependence has been used to determine the surface-potential-barrier height for the whole range of  $x_S \in [0, 1]$ , although other conduction-band offset relations, taking into account terms quadratic in  $x_S$ , have been reported as more appropriate for  $x_S \geq 0.5$  (cf., e.g.,

Refs. 29 and 30). The main reason is that energetic positions of SL surface states, experimentally observed for AlAs-terminated binary  $\text{GaAs}/\text{Al}_x\text{Ga}_{1-x}\text{As}$  SL's (i.e., for  $x_S = 1$ ), have been well reproduced by model calculations using *just* the above *linear* relation for the surface potential step.<sup>22,23</sup> In addition, the obtained surface electronic structure (cf. Sec. IV A) appears to be less sensitive to the exact height of the terminating potential barrier for  $x_S \geq 0.5$  as compared to  $x_S \leq 0.5$ —in this respect, the precise form of the  $V_S(x_S)$  dependence for higher values of  $x_S$  seems not to be that crucial for the present consideration.<sup>31</sup>

##### A. Localized surface states

The resulting surface electronic structure is presented in Fig. 2. As can be seen, the SL has been designed to exhibit an energy spectrum consisting of two minibands of a comparable width, separated by a relatively narrow minigap. Such a bulk band structure appears to be desirable for certain infrared applications of biperiodic SL's, as reported in Ref. 3.

Due to SL termination, the energy levels appear also inside the minigap regions, and they correspond to the states localized at the SL/substrate interface, i.e., to the SL surface states.<sup>32</sup> As follows from Fig. 2, their existence and energy position within a minigap critically depend on the sequence of SL layers approaching the surface. In general, for the surface potential step different from the SL barrier height, eight nonequivalent terminating configurations of SL layers can be distinguished. However, no surface states occur—within the considered energy range—for the wider SL barrier (i.e., layer  $B$ ) being in contact with the substrate. The remaining six SL layer sequences result in distinct surface-state-energy curves as a function of  $x_S$  (i.e., as a function of  $V_S$ ). It is interesting to note that surface states corresponding to the substrate/ $DABC \dots$  and substrate/ $DCBA \dots$  configurations (i.e., for SL terminated at the narrower-barrier layer—cf. Fig. 1) are almost insensitive to the substrate parameters [cf. Fig. 2(c)] and, therefore, seem to originate solely due to the SL potential truncation.

It should be pointed out, however, that particular surface states differ not only in the energy position, but also in their localization properties, as clearly shown in Figs. 3 and 4. The degree of surface-state confinement to the SL end can be conveniently measured by the ratio  $R$  of maxima of its squared wave function in two subsequent (e.g., the second and the first) SL periods, thus describing the surface-state wave function damping towards the SL bulk. As an example, values of  $R$  for surface states corresponding to the substrate/ $ABCD \dots$  and substrate/ $CBAD \dots$  sequences are given in Table I, indicating a strong dependence of the localization factor on the surface level position relative to the bulk band edges. To be more specific, surface states lying close to a miniband exhibit  $R \leq 1$ , hence extend over several layers of the SL, while those well separated from the miniband edges become almost completely confined to the outermost SL period with  $R$  smaller than 0.1. This is illustrated in Fig. 3 for a surface state corresponding to the substrate/ $ABCD \dots$  configuration, emerging from the upper bulk miniband at  $x_S \leq 0.75$  [cf. Fig. 2(a)]. It is also in correspondence with similar findings for binary SL's.<sup>13–15</sup>

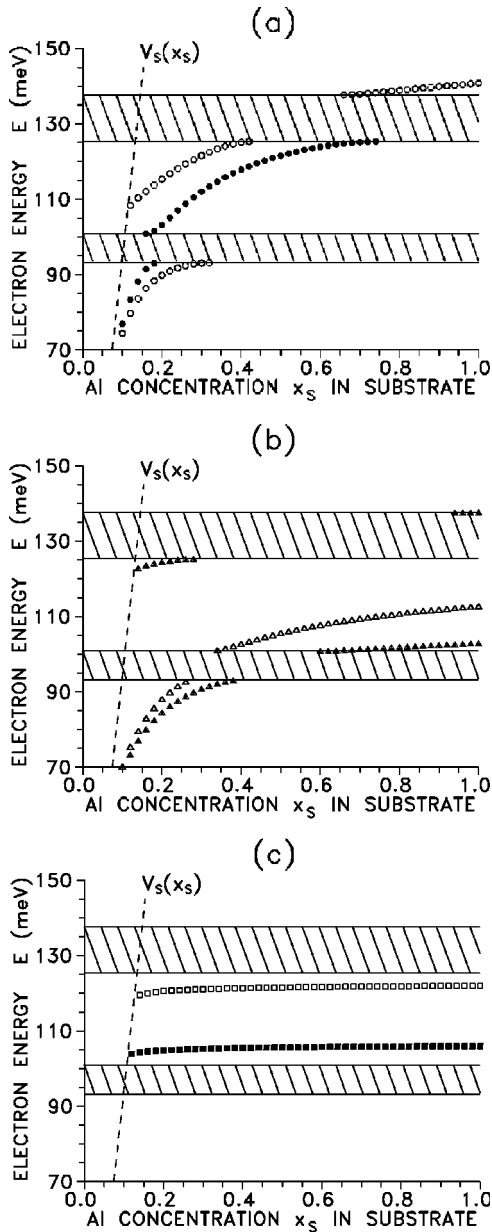


FIG. 2. Surface electronic structure of a double-well GaAs/Al<sub>0.5</sub>Ga<sub>0.5</sub>As SL with  $d_A=40$  Å,  $d_B=25$  Å,  $d_C=45$  Å, and  $d_D=15$  Å, terminated by an Al <sub>$x_S$</sub> Ga<sub>1- $x_S$</sub> As substrate with a variable Al concentration  $x_S$ , for different terminating configurations of SL layers: (a) substrate/ABCD... (full dots) and substrate/ADCB... (open circles), (b) substrate/CDAB... (full triangles) and substrate/CBAD... (open triangles), and (c) substrate/DCBA... (full squares) and substrate/DABC... (open squares). Shaded areas correspond to SL minibands, while dashed lines denote variation of the surface potential barrier height  $V_S(x_S)$ .

In a double-well SL, however, surface states can be additionally differentiated in view of their spatial localization within the SL period. Indeed, they may be either selectively confined to one of the SL wells or distributed over the whole SL basis, as can be seen in Fig. 4. To describe the different cases, the ratio  $Q$  of squared surface-state wave-function maxima in the outermost-but-one and the outermost SL well (i.e., layer-C-to-layer-A or layer-A-to-layer-C; cf. Fig. 1) has been introduced. In Table I, values of  $Q$  are collected for surface states corresponding to the substrate/ABCD... and

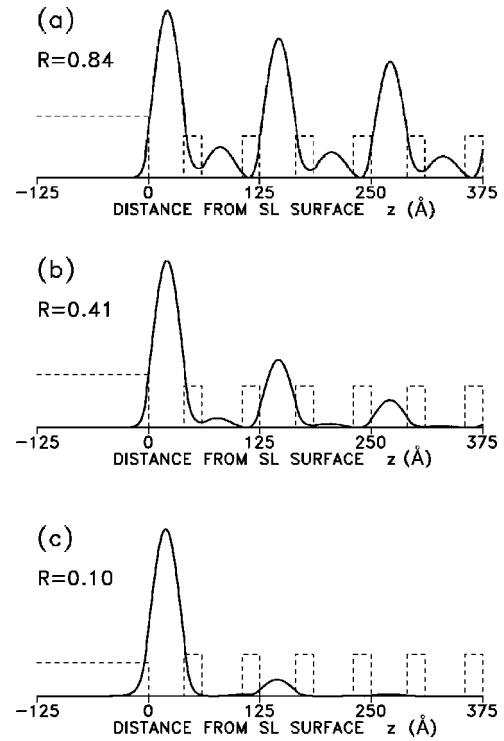


FIG. 3. Squared wave functions (normalized to reach a maximum value of 1) of surface states from the upper branch of a surface-state-energy curve corresponding to the substrate/ABCD... configuration of the considered double-well SL, for different substrate parameters: (a)  $x_S=0.75$ , (b)  $x_S=0.65$ , and (c)  $x_S=0.40$  [cf. Fig. 2(a)]. Localization factor  $R$  gives the ratio of maxima in the second and first SL periods. Dashed lines depict schematically the underlying potential profiles.

substrate/CBAD... configurations. It can be concluded that, in general, surface states localize predominantly in the terminating SL well (being the narrower or wider one for the substrate/ABCD... and substrate/CBAD... sequence, respectively). An interesting exception is seen, for instance, for the substrate/ABCD... case at  $0.15 \leq x_S \leq 0.18$ , when the surface-state wave functions for both branches of the surface-state-energy curve exhibit the most pronounced maximum within the outermost-but-one SL well, i.e., layer C, with  $Q > 1$  [cf. Table I and Fig. 4(c)]. This is due to the proximity of the lower bulk miniband, which originates from the eigenstates of wider SL wells, i.e., is formed by the states confined mostly to layer C. A similar behavior can also be noticed for the substrate/CDAB... sequence: The SL is terminated then at the wider well (layer C), while two branches of the surface-state-energy curve appear near the upper miniband [cf. Fig. 2(b)], originating from the eigenstates of narrower SL wells (layer A). This results again in surface states confined predominantly to the outermost-but-one SL well (layer A).

Another feature of the surface electronic structure of polytype SL's, which contrasts with binary SL's, is the possibility of surface-state existence for the substrate identical to SL barriers (cf. Refs. 15 and 16 for a general discussion of this effect). This peculiarity is indeed seen for the considered bi-periodic SL, with well-defined surface states occurring at  $x_S=0.5$  for the substrate/ABCD... as well as substrate/CBAD... configurations<sup>33</sup> (cf. Fig. 2). It should be empha-

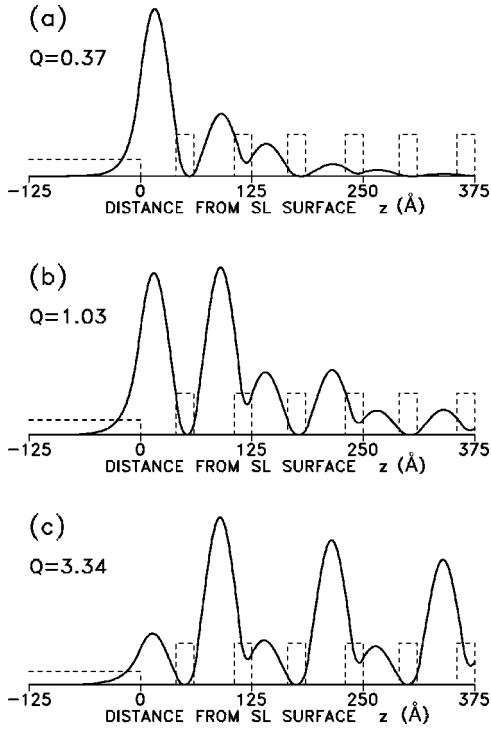


FIG. 4. Squared wave functions (normalized to reach a maximum value of 1) of surface states from the upper branch of a surface-state-energy curve corresponding to the substrate/*ABCD*... configuration of the considered biperiodic SL, for different substrate parameters: (a)  $x_S=0.20$ , (b)  $x_S=0.18$ , and (c)  $x_S=0.16$  [cf. Fig. 2(a)]. Confinement factor  $Q$  gives the ratio of maxima in the outermost-but-one and the outermost SL well (i.e., layer-*C*–to–layer-*A*). Dashed lines depict schematically the underlying potential profiles.

sized that the substrate identical to SL barriers often constitutes the conditions preferred from the grower's point of view, as only two different materials are used then to grow the whole structure. On the other hand, such a particular SL potential truncation, without perturbation of the outermost SL period, is also interesting from the fundamental point of view, being reminiscent of the so-called Shockley terminating conditions.<sup>34</sup> This paves a way for an experimental investigation of the existence and properties of classical Shockley-type surface states using a biperiodic semiconductor SL, in a similar manner the Tamm-like states have been observed—for the first time in their pure form—in AlGaAs-based binary SL's.<sup>22,23</sup>

### B. Density-of-states distributions

As can be expected, terminating the SL potential leads also to a redistribution of extended states within SL minibands. In general, the most pronounced DOS modifications at the SL end are found whenever a surface-state-energy curve emerges from the bulk miniband. To illustrate this effect, LDOS distributions have been computed<sup>35</sup> for the substrate/*ADCB*... configuration and different substrate parameters corresponding to  $0 \leq x_S \leq 0.5$  [cf. Fig. 2(a)]. The resulting series of gray-scale LDOS maps over a few outermost SL periods is presented in Fig. 5.

As can be seen, the states forming the lower (upper) miniband are always predominantly localized within wider (narrower) SL wells, which is a purely bulk property of a biperiodic SL, related to the origin of particular minibands (bulk DOS features of SL's with different geometry of a complex basis are thoroughly discussed in Ref. 36). For  $x_S=0.5$  [cf. Fig. 5(a)], when no surface states exist for the substrate/*ADCB*... configuration [cf. the open-circle curve in Fig.

TABLE I. Localization properties of surface states for (a) substrate/*ABCD*... and (b) substrate/*CBAD*... terminating configuration of a double-well GaAs/Al<sub>0.5</sub>Ga<sub>0.5</sub>As SL with  $d_A=40$  Å,  $d_B=25$  Å,  $d_C=45$  Å, and  $d_D=15$  Å, for different Al concentration  $x_S$  in the substrate.  $E_{SS}$  stands for the energy of a surface state (in meV),  $R$  gives the ratio of maxima of the squared surface-state wave function in the second and first SL periods, while  $Q$  denotes the ratio of maxima in the outermost-but-one and the outermost SL well. Upper (lower) row corresponds to the upper (lower) branch of the respective surface-state-energy curve (cf. Fig. 2).

(a)											
$x_S$	0.10	0.16	0.18	0.20	0.30	0.40	0.50	0.60	0.70	0.72	0.74
$E_{SS}$	76.89	91.46	93.06								
		100.90	101.55	103.13	112.02	117.82	121.55	123.90	125.12	125.24	125.31
$R$	0.002	0.113	0.507								
		0.878	0.385	0.194	0.077	0.099	0.165	0.308	0.624	0.724	0.836
$Q$	0.024	0.393	1.254								
		3.345	1.030	0.372	0.032	0.008	0.000	0.032	0.116	0.147	0.185
(b)											
$x_S$	0.10	0.20	0.24	0.26	0.34	0.36	0.40	0.50	0.60	0.80	1.00
$E_{SS}$	70.20	88.08	91.57	92.71							
					101.04	101.52	102.75	105.61	107.79	110.79	112.72
$R$	0.001	0.027	0.120	0.304							
					0.627	0.395	0.219	0.115	0.091	0.078	0.077
$Q$	0.008	0.045	0.109	0.202							
					0.120	0.054	0.016	0.000	0.009	0.021	0.033

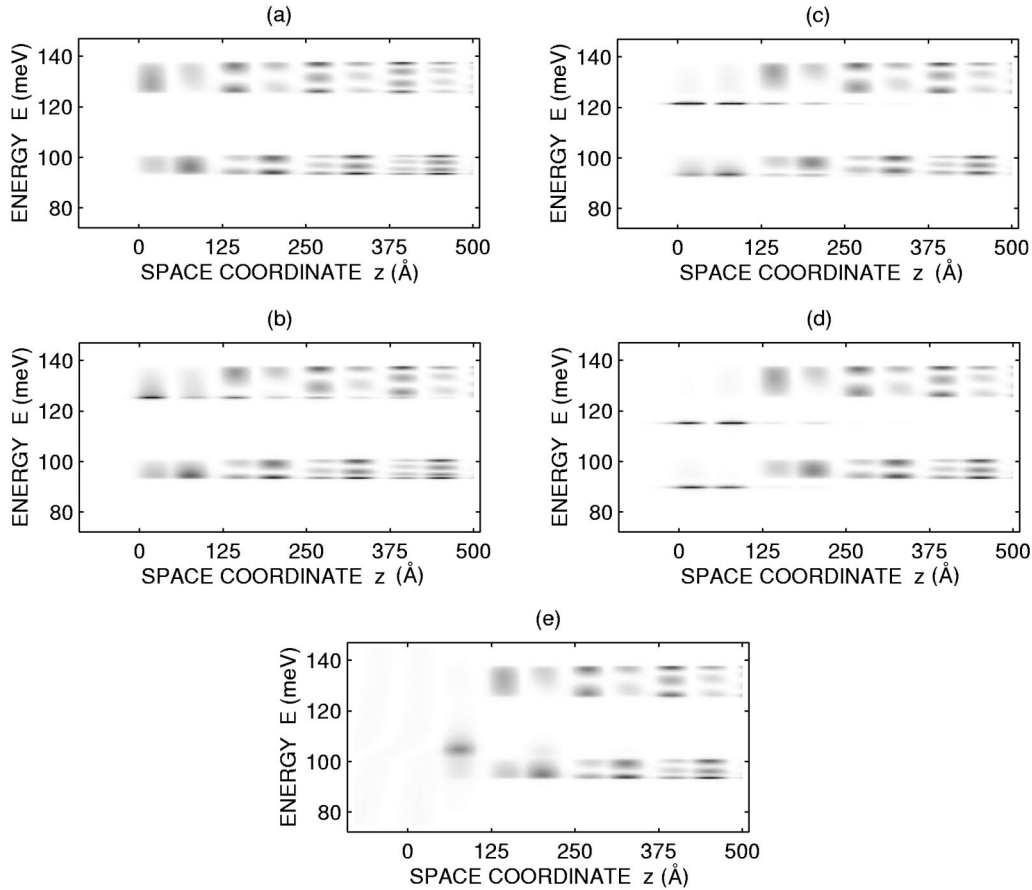


FIG. 5. LDOS distributions for the substrate/*ADCB* ... configuration of a double-well GaAs/Al<sub>0.5</sub>Ga<sub>0.5</sub>As SL with  $d_A=40$  Å,  $d_B=25$  Å,  $d_C=45$  Å, and  $d_D=15$  Å, terminated by an Al <sub>$x_S$</sub> Ga <sub>$1-x_S$</sub> As substrate with different Al concentration  $x_S$ : (a)  $x_S=0.5$ , (b)  $x_S=0.4$ , (c)  $x_S=0.3$ , (d)  $x_S=0.2$ , and (e)  $x_S=0.0$ . The space coordinate  $z$ , measured from the SL/substrate interface at  $z=0$ , ranges over four outermost SL periods. Dark- and light-gray areas correspond to high and low values of LDOS, respectively.

2(a)], the LDOS distribution takes—inside both minibands—an *unperturbed* shape (cf. Ref. 34), characteristic also for binary SL's terminated by a substrate identical to SL barriers.<sup>18,19</sup> More specifically, in the vicinity of the SL surface LDOS vanishes at the miniband edges and exhibits a smooth maximum in the middle, whereas in the subsequent SL periods it shows more and more oscillations within each miniband, reproducing finally, deep inside the SL bulk, a typical divergent behavior at the band edges, in accordance with one-dimensional van Hove-like singularities.

Already for  $x_S=0.4$  [cf. Fig. 5(b)], however, a noticeable rearrangement of states—in particular, an energy shift of LDOS maxima in the subsurface SL layers—takes place within the upper miniband, being associated with the formation of a surface state near the band edge. Essentially the same happens to the lower miniband for  $x_S=0.3$  [cf. Fig. 5(c)] as a result of the second branch of the surface-state-energy curve emerging below this miniband [cf. Fig. 2(a)]. Furthermore, since the upper surface state becomes already well localized for  $x_S=0.3$ , a deficiency of states forming the upper miniband is observed within the outermost SL period, in correspondence with similar findings for binary SL's.<sup>18,19</sup> This effect, reflecting the charge conservation rule, is even more pronounced for  $x_S=0.2$  [cf. Fig. 5(d)], when both surface states are almost completely confined to the subsurface SL period, while the LDOS within both minibands is re-

pelled by one period towards the SL bulk, taking again an unperturbed shape [cf. Fig. 5(d) vs Fig. 5(a)]. In such a case, the outermost double-well basis appears to be decoupled from the rest of an otherwise undisturbed semi-infinite SL, with the LDOS distribution of the whole system resembling a simple superposition of distributions corresponding to the noninteracting subsystems.

Finally, for  $x_S=0$  the substrate becomes identical to SL wells, so the substrate/*ADCB* ... configuration coincides with the substrate/*DCBA* ... one and the actual SL surface is shifted by nearly half a SL period with respect to its original position at  $z=0$  [cf. Fig. 5(e)]. Moreover, since the conduction band lies now entirely above the surface-potential barrier, surface states start to interact with the continuum of states of the substrate. As a result, they cease to exist as truly localized discrete levels, but the corresponding LDOS distributions may still exhibit well-defined features, characteristic for surface resonances. Such a resonance, located above the lower miniband and confined predominantly to the outermost SL well (i.e., to layer *C*) can be clearly recognized in Fig. 5(e). It is interesting to note that its energy position almost coincides with that of a surface state appearing for the substrate/*CBAD* ... sequence and the substrate identical to SL barriers [cf. Fig. 2(b) for  $x_S=0.5$ ]. It means that actually the same surface state/resonance originates while terminating the SL at layer *C* either by a semi-infinite (substrate) or a

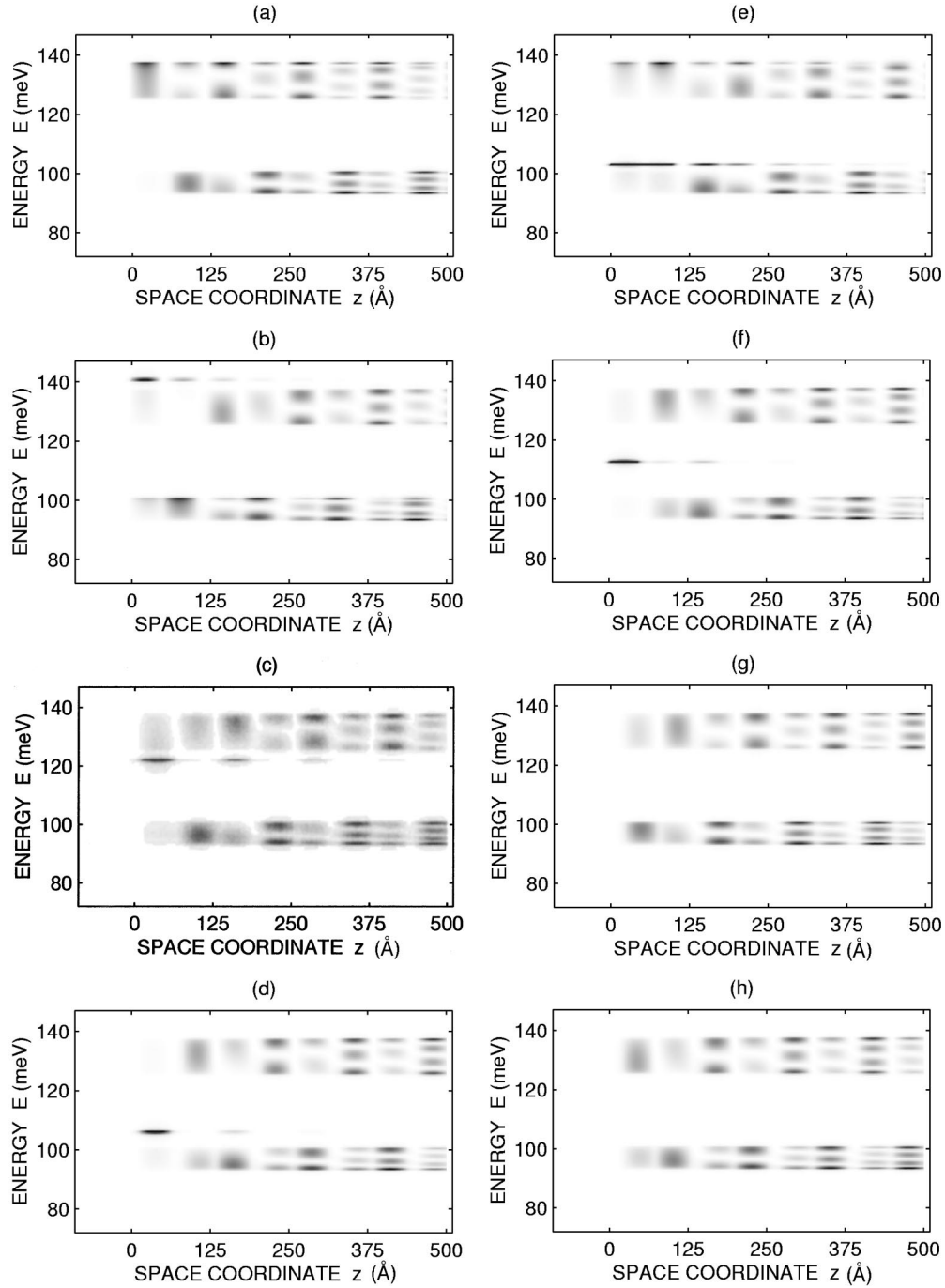


FIG. 6. LDOS distributions of a double-well GaAs/Al<sub>0.5</sub>Ga<sub>0.5</sub>As SL with  $d_A=40$  Å,  $d_B=25$  Å,  $d_C=45$  Å, and  $d_D=15$  Å, terminated by an AlAs substrate, for different configurations of SL layers: (a) substrate/ABCD . . . , (b) substrate/ADCB . . . , (c) substrate/DABC . . . , (d) substrate/DCBA . . . , (e) substrate/CDAB . . . , (f) substrate/CBAD . . . , (g) substrate/BCDA . . . , and (h) substrate/BADC . . . . The space coordinate  $z$ , measured from the SL/substrate interface at  $z=0$ , ranges over four outermost SL periods. Dark- and light-gray areas correspond to high and low values of LDOS, respectively.

finite-width (layer  $D$ ) barrier of the same height. This supports a conclusion of Sec. IV A that it indeed occurs solely due to the SL potential truncation. It should be stressed here that the possibility of formation of well-defined surface resonances is a unique feature of semi-infinite SL's with multilayer basis, as they never occur in terminated binary SL's.<sup>15</sup>

Similar LDOS perturbations have been, in fact, also noticed for the substrate/ABCD . . . terminating configuration. Then, however, because of a surface state crossing the lower

miniband for  $0.12 \leq x_S \leq 0.22$  [cf. Fig. 2(a)], even slight changes to the substrate composition within this narrow range dramatically influence the space-charge distribution at the SL end. Pronounced LDOS modifications are additionally seen for the SL terminated by a substrate identical to either SL wells or SL barriers.

For completeness, differences in DOS characteristics for various possible configurations of SL layers have been examined for fixed substrate parameters. Results obtained for the AlAs substrate (i.e., for  $x_S=1$ ) are presented in Fig. 6. It

is clear that the LDOS distribution near the SL surface critically depends on the type of layer by which the SL sequence ends. Indeed, a direct comparison of Figs. 6(a) and 6(e), Figs. 6(b) and 6(f), Figs. 6(c) and 6(g), or Figs. 6(d) and 6(h), respectively, indicates that adding half a SL period modifies quite substantially space-charge distributions at the SL end by affecting the surface-state existence condition (see also Fig. 2). As a matter of fact, only SL's terminated at layer  $B$  (i.e., when the wider barrier is in contact with the AIAs substrate) exhibit unperturbed LDOS characteristics within both minibands [cf. Figs. 6(g) and 6(h)]. This should be taken into account when considering specific applications of double-well SL's.

## V. CONCLUDING REMARKS

As has been shown, the energy spectrum and localization properties of surface states of a biperiodic SL, as well as the corresponding LDOS distributions, critically depend on the choice of substrate and the configuration of SL layers approaching the surface. In particular—in contrast with standard (i.e., binary) SL's—surface states (resonances) can appear while terminating a double-well SL by a substrate identical to SL barriers (wells). Furthermore, they can be predominantly confined to the outermost-but-one rather than

the outermost SL well layer, which is also never the case in standard SL's.

Owing to some peculiarities of surface-localized levels as compared to SL bulk states, their presence might have important consequences for various optoelectronic characteristics of double-well SL's, as it happens for binary SL's.<sup>37</sup> Therefore, the existence of surface states in biperiodic SL's and an opportunity of tailoring their unusual properties merits further theoretical and experimental investigation. Having in mind different applications of double-well SL's, the indicated possibility to arrange various LDOS distributions at the SL end is also of considerable interest. To be more specific, by an appropriate choice of terminating conditions, the spatial overlap of states forming particular SL minibands can be tuned in the subsurface SL region, hence the corresponding interminiband optical transition rates can be modified in a controlled manner.

## ACKNOWLEDGMENTS

We would like to thank Dr. El Houssaine El Boudouti from the University of Oujda, Morocco, for providing us with a code for density-of-states computations. One of us (R.K.) gratefully acknowledges support by the University of Wrocław within the Grant No. 2315/W/IFD/99.

\*Corresponding author. E-mail: rku@ifd.uni.wroc.pl

<sup>1</sup>P.-F. Yuh and K.L. Wang, Phys. Rev. B **38**, 13 307 (1988).

<sup>2</sup>F.M. Peeters and P. Vasilopoulos, Appl. Phys. Lett. **55**, 1106 (1989).

<sup>3</sup>P. Vasilopoulos, F.M. Peeters, and D. Aitelhabeti, Phys. Rev. B **41**, 10 021 (1990).

<sup>4</sup>G. Ihm, S.K. Noh, J.I. Lee, and T.W. Kim, Superlattices Microstruct. **12**, 155 (1992).

<sup>5</sup>H.M. Guerrero, G.H. Cocolletzi, and S.E. Ulloa, J. Appl. Phys. **78**, 2541 (1995).

<sup>6</sup>L. Fernández-Alvarez, G. Monsivais, and V.R. Velasco, J. Phys.: Condens. Matter **8**, 8859 (1996).

<sup>7</sup>K.K. Choi, B.F. Levine, C.G. Bethea, J. Walker, and R.J. Malik, Phys. Rev. Lett. **59**, 2459 (1987).

<sup>8</sup>H. Schneider, K. Kawashima, and K. Fujiwara, Phys. Rev. B **44**, 5943 (1991).

<sup>9</sup>F. Agulló-Rueda, H.T. Grahn, and K. Ploog, J. Appl. Phys. **79**, 8106 (1996).

<sup>10</sup>K. Fujiwara, S. Hinooda, and K. Kawashima, Appl. Phys. Lett. **71**, 113 (1997).

<sup>11</sup>M. Takeuchi, T. Imanishi, D. Ushijima, K. Kawashima, and K. Fujiwara, Physica E **2**, 303 (1998).

<sup>12</sup>A. Kristensen, P.E. Lindelof, C.B. Sørensen, and A. Wacker, Semicond. Sci. Technol. **13**, 910 (1998).

<sup>13</sup>P. Masri, Surf. Sci. Rep. **19**, 1 (1993).

<sup>14</sup>J. Arriaga, F. García-Moliner, and V.R. Velasco, Prog. Surf. Sci. **42**, 271 (1993).

<sup>15</sup>M. Stęślička, Prog. Surf. Sci. **50**, 65 (1995).

<sup>16</sup>E.-H. El Boudouti, B. Djafari-Rouhani, A. Akjouj, L. Dobrzynski, R. Kucharczyk, and M. Stęślička, Phys. Rev. B **56**, 9603 (1997).

<sup>17</sup>R. Kucharczyk, M. Stęślička, A. Akjouj, B. Djafari-Rouhani, L. Dobrzynski, and E.-H. El Boudouti, Phys. Rev. B **58**, 4589 (1998).

<sup>18</sup>E.-H. El Boudouti, R. Kucharczyk, and M. Stęślička, Czech. J. Phys. **43**, 899 (1993).

<sup>19</sup>R. Kucharczyk and M. Stęślička, Prog. Surf. Sci. **46**, 225 (1994).

<sup>20</sup>E.-H. El Boudouti, B. Djafari-Rouhani, A. Akjouj, and L. Dobrzynski, Phys. Rev. B **54**, 14 728 (1996).

<sup>21</sup>B. Djafari-Rouhani and L. Dobrzynski, Solid State Commun. **62**, 609 (1987).

<sup>22</sup>H. Ohno, E.E. Mendez, J.A. Brum, J.M. Hong, F. Agulló-Rueda, L.L. Chang, and L. Esaki, Phys. Rev. Lett. **64**, 2555 (1990).

<sup>23</sup>H. Ohno, E.E. Mendez, A. Alexandrou, and J.M. Hong, Surf. Sci. **267**, 161 (1992).

<sup>24</sup>It is worth noticing that a distinct depth of the wells or height of the barriers comprising the double-well basis would be an unnecessary complication of the considered system, as the basic features of its electronic structure are determined by the relative position of the eigenstates of the corresponding isolated wells as well as the relative barrier coupling strengths rather than by all the details of the underlying potential shape.

<sup>25</sup>Since we are interested in general trends rather than a complete picture, our considerations are restricted here to the two lowest conduction minibands. On the other hand, this is, in fact, the energy range most relevant for various SL applications.

<sup>26</sup>R. Kucharczyk, U. Freking, P. Krüger, and J. Pollmann, Surf. Sci. (submitted).

<sup>27</sup>D.M. Wood and A. Zunger, Phys. Rev. B **53**, 7949 (1996).

<sup>28</sup>S. Krylyuk, D.V. Korbutyak, V.G. Litovchenko, R. Hey, H.T. Grahn, and K.H. Ploog, Appl. Phys. Lett. **74**, 2596 (1999).

<sup>29</sup>R.K. Gug and W.E. Hagston, Appl. Phys. Lett. **74**, 254 (1999).

<sup>30</sup>E.H. Li, Physica E **5**, 215 (2000).

<sup>31</sup>It is nevertheless fair to say that the results obtained for  $x_S \geq 0.5$  are less reliable than those for  $x_S \leq 0.5$ .

<sup>32</sup>It should be pointed out that true surface states can only exist in the energy range below the surface potential barrier height  $V_S$ —otherwise they get in resonance with the continuum of

states of the substrate and lose the bound character of discrete levels. Such surface resonances are discussed in Sec. IV B.

<sup>33</sup>Please note that in such a case these coincide with the substrate/*DABC* . . . and substrate/*DCBA* . . . sequences, respectively.

<sup>34</sup>S.G. Davison and M. Stęślicka, *Basic Theory of Surface States* (Clarendon Press, Oxford, 1992).

<sup>35</sup>A small imaginary part of energy is assumed in LDOS computa-

tions in order to lift the singular character of discrete surface levels, so they can be represented as narrow peaks of a finite height.

<sup>36</sup>R. Kucharczyk, M. Stęślicka, B. Brzostowski, and B. Djafari-Rouhani, *Physica E* **5**, 280 (2000).

<sup>37</sup>J. Zhang, S.E. Ulloa, and W.L. Schaich, *Phys. Rev. B* **43**, 9865 (1991).